CrystEngComm

Cite this: *CrystEngComm*, 2012, **14**, 3478

www.rsc.org/crystengcomm

PAPER

Syntheses, crystal structures, thermal stabilities and luminescence of two metal phosphonates†

Ruibiao Fu,* Shengmin Hu and Xintao Wu

Received 27th February 2012, Accepted 5th March 2012
DOI: 10.1039/c2ce25279a

Hydrothermal reactions of Zn(II) or Pb(II) ions with 4-pyridyl-$CH_2N(CH_2COOH)(CH_2PO_3H_2)$ (H_3L) afforded two metal phosphonates, namely, $[Zn_3(L)_2]\cdot 2H_2O$ (**1**) and $[Pb_3(L)_2(H_2O)_2]\cdot H_2O$ (**2**). Compound **1** is a 3D pillared framework in which $[ZnO_4]$ tetrahedra and $[ZnO_3N_2]$ trigonal-bipyramids are connected by L^{3-} anions with heptadentate modes. In **2**, L^{3-} anions exhibit pentadentate modes to combine Pb(II) ions into a complicated 2D hybrid layer, resulting in the non-coordinated pyridine rings being sandwiched between the layers. Solid **1** is thermally stable up to 350 °C under an air atmosphere and displays bright purple–blue luminescence, and the luminescent intensity of the hydrated solid **1** can be weakened by nitrobenzene.

Introduction

Metal phosphonates have gained great research interest not only for their structural and compositional diversities but also for their potential applications as porous materials, ion-exchangers, non-linear optics, catalysts, Langmuir–Blodgett films, molecular sensors, non-linear optics, and so on.[1] Therefore, a variety of intriguing metal phosphonates have been synthesized during the past five years.[2–4] The strategy of attaching additional groups such as amine, hydroxyl, imidazole, carboxylate, pyridyl, triazole, sulfonate, thienyl and benzimidazol groups to the phosphonic acids has been proven to be an effective way for the isolation of a number of metal phosphonates with interesting structures and properties.[5–9] For example, heterobimetallic U(VI)/M(II) phosphonates adopt cubic 3D network structures with large cavities approximately 16 Å in diameter,[7c] and Co(2-pmp)$(H_2O)_2$ shows reversible changes of structures and magnetic behaviors upon the dehydration–hydration process.[5c] This is mainly due to additional groups not only being able to enrich coordination modes, but also being able to improve the solubility and crystallinity of metal phosphonates. In this regard, 4-pyridyl-$CH_2N(CH_2COOH)(CH_2PO_3H_2)$ (H_3L) featuring a connection of phosphonate, carboxylate and pyridyl groups *via* an $N(CH_2)_3$ moiety, has been synthesized. Such a multi-functional ligand would adopt diversified coordination modes with metal ions to form many interesting metal phosphonates. In this paper, we report the synthesis, crystal structures, thermal stabilities and luminescence of two metal phosphonates: $[Zn_3(L)_2]\cdot 2H_2O$ (**1**) and $[Pb_3(L)_2(H_2O)_2]\cdot H_2O$ (**2**).

State Key Laboratory of Structural Chemistry, Fujian Institute of Research on the Structure of Matter, Chinese Academy of Science, Fuzhou, Fujian, 350002 China. E-mail: wxt@fjirsm.ac.cn; Fax: + 86-591-83714946; Tel: + 86-591-83792837

† Electronic supplementary information (ESI) available: IR spectra, TGA curves, powder XRD patterns and luminescent spectra. CCDC reference numbers 831048 (**1**) and 831049 (**2**). For ESI and crystallographic data in CIF or other electronic format see DOI: 10.1039/c2ce25279a

Experimental

Materials and instrumentation

4-Pyridyl-$CH_2N(CH_2COOH)(CH_2PO_3H_2)$ was prepared by N-alkylation reaction. Other chemicals were obtained from commercial sources without further purification. Elemental analyses were carried out with a Vario EL III element analyzer. Infrared spectra were obtained on a Nicolet Magna 750 FT-IR spectrometer. Photoluminescent properties were investigated in the solid state at room temperature with a F-7000 FL spectrophotometer and an Edinburgh FLS920 fluorescence spectrometer. Thermogravimetric analysis (TGA) was performed on a Netzsch STA449C at a heating rate of 10 °C min^{-1} from room temperature to 800 °C under an air gas flow. Powder XRD patterns were acquired on a DMAX-2500 diffractometer using Cu-Kα radiation under an ambient environment. The BET surface area at 78 K was obtained on an ASAP 2020 specific surface area and porosity analyzer. The ESI mass spectrum was recorded on a DECAX-30000 LCQ Deca XP spectrometer.

Synthesis of $[Zn_3(L)_2]\cdot 2H_2O$ (1). A mixture of H_3L (0.1026 g, 0.3943 mmol), $Zn(CH_3COO)_2\cdot 2H_2O$ (0.0815 g, 0.371 mmol), and triethylamine (0.45 mL, 3.2 mmol) in 8.0 mL distilled water was sealed into a Parr Teflon-lined autoclave (23 mL) and heated at 180 °C for 120 h. After slow cooling to room temperature with a rate of 0.056 °C min^{-1}, the pH value of the final mixture was 6.60 and colorless crystals were obtained as a homogenous phase based on powder XRD patterns. Yield: 0.0684 g (74%). Anal. Calc. for $C_{18}H_{24}N_4O_{12}P_2Zn_3$: C 28.96, H 3.24, N 7.51%.

Found: C 28.76, H 3.27, N 7.34%. IR (KBr pellet, cm^{-1}): 3439m(υ_{O-H}), 2946w(υ_{C-H}), 2906w, 2849w, 1606s(υ_{CO}), 1589s, 1444m, 1436m, 1429m, 1410m, 1334w, 1306w, 1239w, 1223w, 1136m($\upsilon_{P=O}$), 1112s(υ_{P-O}), 1097s(υ_{P-O}), 1079s(υ_{P-O}), 1026m(υ_{P-O}), 1008m(υ_{P-O}), 988m(υ_{P-O}), 934w, 892w, 844w, 807w, 768m, 641m.

Synthesis of $[Pb_3(L)_2(H_2O)_2]\cdot H_2O$ (2). A mixture of H_3L (0.0515 g, 0.1979 mmol), $Pb(CH_3COO)_2\cdot 3H_2O$ (0.0563 g, 0.1484 mmol), and triethylamine (0.2 mL, 1.4 mmol) in 8.0 mL distilled water was sealed into a Parr Teflon-lined autoclave (23 mL) and heated at 105 °C for 120 h. After slow cooling to room temperature with a rate of 0.030 °C min^{-1}, the pH value of the final mixture was 5.68 and colorless needle-like crystals were obtained as a homogenous phase based on powder XRD patterns. Yield: 0.0300 g (51%). Anal. Calc. for $C_{18}H_{26}N_4O_{13}P_2Pb_3$: C 18.17, H 2.20, N 4.71%. Found: C 17.56, H 2.12, N 4.56%. IR (KBr pellet, cm^{-1}): 3317m, 2951w(υ_{C-H}), 2942w(υ_{C-H}), 2903w, 2892, 2855w, 2845w, 2807w, 1599m, 1587m, 1563m, 1451m, 1420m, 1379m, 1352w, 1326w, 1227w, 1215w, 1115m($\upsilon_{P=O}$), 1106m(υ_{P-O}), 1098m(υ_{P-O}), 1086m(υ_{P-O}), 1075m(υ_{P-O}), 1039s(υ_{P-O}), 1002m(υ_{P-O}), 957m, 944m, 874w, 797m, 640m, 551m.

Heating treatment. Solids **1-200**, **1-250** and **1-300** were obtained after polycrystalline **1** was heated at 200, 250 and 300 °C for two hours under an air atmosphere, respectively, and then naturally cooled to room temperature, while solid **1-350** was obtained after polycrystalline **1** was heated from room temperature to 350 °C at a heating rate of 5.5 °C min^{-1} under an air atmosphere, and then cooled immediately to room temperature. Anal. Calc. for solid **1-350** ($C_{18}H_{20}N_4O_{10}P_2Zn_3$): C 30.43, H 2.84, N 7.89%. Found: C 29.47, H 3.43, N 7.78%.

X-ray crystallography

X-ray data for **1–2** were collected at 293(2) K on a Rigaku Mercury CCD/AFC diffractometer using graphite-monochromated Mo-Kα radiation (λ(Mo-Kα) = 0.71073 Å). Data of **1–2** were reduced with CrystalClear v1.3. These structures were solved by direct methods and refined by the full-matrix least-squares techniques on F^2 using SHELXTL-97.[10] All non-hydrogen atoms were treated anisotropically. Hydrogen atoms of carbon atoms were generated geometrically. No attempts were performed to locate hydrogen atoms of water molecules in **1**, while hydrogen atoms of water molecules in **2** were from a difference Fourier map and fixed with O–H = 0.96 Å. Crystallographic data for compounds **1–2** are summarized in Table 1. The high wR_2 value of compound **1** is possibly due to the weak diffraction intensity. Selected bond lengths and angles for compounds **1** and **2** are listed in Tables 2 and 3, respectively. Hydrogen bond lengths and angles for compound **2** are listed in Table 4. CCDC 831048 (**1**) and 831049 (**2**).†

Results and discussion

Syntheses and characterization

Compounds **1–2** were synthesized by the reaction mixtures of $Zn(CH_3COO)_2$ or $Pb(CH_3COO)_2$, H_3L and triethylamine under hydrothermal conditions, and solids **1–2** were satisfactorily characterized by single-crystal X-ray diffraction, powder XRD, IR and elemental analyses (EA). The bands centered at 3439 (for **1**) and 3317 cm^{-1} (for **2**), are attributed to the O–H stretching vibration of water molecules. During synthesis process, the pH value of the reaction mixture was adjusted by different amounts of triethylamine. Solid **1** can be obtained with a pH value in a broad range of 3.16–10.17 (Fig.1). However, solid **2** can only be synthesized with a pH value in a narrow range of 4.45–5.68.

Structural descriptions

The asymmetric unit of **1** contains three crystallographically independent Zn(II) ions, two L^{3-} anions and two free water molecules (Fig. 2a). Zn1 is surrounded by four L^{3-} anions into a distorted [ZnO_4] tetrahedral coordination geometry. Two L^{3-} anions interact with Zn1 through two phosphonate oxygen atoms (O1, O6), while the other two L^{3-} anions contact Zn1 *via* two carboxylate oxygen atoms (O4b, O9a). The τ value (0.77) reveals that Zn2 is in a distorted [ZnO_3N_2] trigonal-bipyramidal geometry, which is surrounded by three L^{3-} anions.[11] It is attractive that one L^{3-} anion is chelated to Zn2 *via* one nitrogen donor (N2c), one phosphonate (O3c) and one carboxylate oxygen atoms (O5c), resulting in a Zn–O–P–C–N and a Zn–O–C–C–N ring, while the other two L^{3-} anions contact Zn2 through one phosphonate oxygen atom (O2) and one nitrogen donor (N1d) of pyridine, respectively. The geometry around Zn3 is nearly in between square pyramidal and trigonal-bipyramidal geometry based on the τ value (0.48). The interactions of Zn3 and three L^{3-} anions are similar to those of Zn2. The bond lengths of Zn–O and Zn–N are in the range of 1.920(7)–2.058(6) and 2.093(7)–2.271(7) Å, respectively. On the other hand, the L^{3-} anion exhibits a heptadentate mode to combine five Zn(II) ions through three phosphonate and two carboxylate oxygen atoms along with two nitrogen donors. Thus, zinc ions are interconnected by phosphonate and carboxylate groups, as well as nitrogen atoms into a 2D hybrid layer. The layers are further linked by pyridine groups into a 3D pillared framework containing channels along the *b* axis and the channel is occupied by the free water molecules.

The asymmetric unit of **2** also consists of three crystallographically independent Pb(II) ions, two L^{3-} anions, and two coordinated and one free water molecules (Fig. 3a). Pb1 is surrounded by two L^{3-} anions and one coordinated water molecule (O11) into a distorted ψ-PbO_4N octahedral geometry with the lone pair occupying the sixth coordination site. The same as in **1**, one L^{3-} anion is chelated to Pb1 *via* one nitrogen donor (N1), one phosphonate (O1) and one carboxylate oxygen atom (O4), resulting in a Pb–O–P–C–N and a Pb–O–C–C–N ring. The N1 atom locates the polar site of ψ-PbO_4N octahedron, while the other two basal sites are occupied by another phosphonate oxygen atom (O6a) from the second L^{3-} anion and the coordinated water molecule (O11). Pb2 is in a distorted ψ-PbO_5 octahedral geometry, which is defined by three phosphonate oxygen atoms (O1, O2b, O7) and one carboxylate oxygen donor (O4c) from four L^{3-} anions, as well as one coordinated water molecule (O12). The two polar sites of the ψ-PbO_5 octahedron are occupied by O1 and the lone pair, respectively. The Pb3 is surrounded by three L^{3-} anions, resulting in a distorted ψ-PbO_4N octahedral

Table 1 Crystallographic data for compounds **1** and **2**

Compounds	**1**	**2**
Formula	$C_{18}H_{24}N_4O_{12}P_2Zn_3$	$C_{18}H_{26}N_4O_{13}P_2Pb_3$
FW	746.46	1189.94
Space group	$P2_1/c$	$P\bar{1}$
a/Å	16.566(15)	8.9939(2)
b/Å	8.573(8)	10.8591(5)
c/Å	18.719(17)	14.3633(3)
α (°)	90	88.893(6)
β (°)	101.70(2)	74.348(5)
γ (°)	90	84.146(5)
V/Å^3	2603(4)	1343.69(7)
Z	4	2
T/K	293(2)	293(2)
Measured/unique/observed reflections	19359/5913/4458	16630/6131/5464
D_{calcd} (g cm^3)	1.905	2.941
μ/mm^{-1}	2.933	18.940
GOF on F^2	1.074	1.054
R_{int}	0.0591	0.0342
$R_1{}^a$ [$I > 2\sigma(I)$]	0.0880	0.0268
w$R_2{}^b$ [all data]	0.2228	0.0507

^{a} $R_1 = \sum(||F_o| - |F_c||)/\sum|F_o|$. ^{b} $wR_2 = \{\sum w[(F^2_o - F^2_c)]/\sum w[(F^2_o)^2]\}^{0.5}$.

Table 2 Selected bond lengths (Å) and angles (°) for **1**[a]

Zn(1)–O(1)	1.953(6)	Zn(2)–O(3)^c	1.978(6)
Zn(1)–O(4)^b	2.026(6)	Zn(2)–O(5)^c	2.036(6)
Zn(1)–O(6)	1.920(7)	Zn(3)–N(3)^f	2.101(8)
Zn(1)–O(9)^a	1.958(6)	Zn(3)–N(4)^f	2.251(8)
Zn(2)–N(1)^d	2.093(7)	Zn(3)–O(7)	1.930(6)
Zn(2)–N(2)^c	2.271(7)	Zn(3)–O(8)^e	2.030(7)
Zn(2)–O(2)	1.967(6)	Zn(3)–O(10)^e	2.058(6)
O(1)–Zn(1)–O(4)^b	114.2(2)	O(2)–Zn(2)–O(3)^c	127.0(2)
O(1)–Zn(1)–O(6)	104.3(3)	O(2)–Zn(2)–O(5)^c	111.6(3)
O(1)–Zn(1)–O(9)^a	108.2(3)	O(3)^c–Zn(2)–O(5)^c	119.5(3)
O(4)^b–Zn(1)–O(6)	104.7(3)	N(3)^f–Zn(3)–N(4)^f	161.0(3)
O(4)^b–Zn(1)–O(9)^a	115.2(3)	N(3)^f–Zn(3)–O(7)	96.9(3)
O(6)–Zn(1)–O(9)^a	109.5(3)	N(3)^f–Zn(3)–O(8)^e	90.7(3)
N(1)^d–Zn(2)–N(2)^c	165.5(3)	N(3)^f–Zn(3)–O(10)^e	91.2(3)
N(1)^d–Zn(2)–O(2)	99.2(3)	N(4)^f–Zn(3)–O(7)	102.1(3)
N(1)^d–Zn(2)–O(3)^c	92.7(3)	N(4)^f–Zn(3)–O(8)^e	84.2(3)
N(1)^d–Zn(2)–O(5)^c	91.7(3)	N(4)^f–Zn(3)–O(10)^e	79.0(3)
N(2)^c–Zn(2)—O(2)	93.9(2)	O(7)–Zn(3)–O(8)^e	109.8(3)
N(2)$^{c-}$–Zn(2)–O(3)^c	84.2(2)	O(7)–Zn(3)–O(10)^e	117.1(3)
N(2)^c–Zn(2)–O(5)^c	77.6(2)	O(8)^e–Zn(3)–O(10)^e	132.4(3)

[a] Symmetry codes: (a) $x, y - 1, z$; (b) $-x, y - 1/2, -z + 1/2$; (c) $-x, y + 1/2, -z + 1/2$; (d) $-x, -y + 1, -z + 1$; (e) $-x - 1, y - 1/2, -z + 1/2$; (f) $-x - 1, -y + 1, -z + 1$.

Table 3 Selected bond lengths (Å) and angles (°) for **2**[a]

Pb(1)–N(1)	2.743(4)	Pb(2)–O(7)	2.711(3)
Pb(1)–O(1)	2.642(3)	Pb(2)–O(12)	2.676(4)
Pb(1)–O(4)	2.619(3)	Pb(3)–N(3)	2.608(4)
Pb(1)–O(6)^a	2.389(3)	Pb(3)–O(2)^b	2.713(3)
Pb(1)–O(11)	2.565(3)	Pb(3)–O(3)	2.523(3)
Pb(2)–O(1)	2.440(3)	Pb(3)–O(8)	2.381(3)
Pb(2)–O(2)^b	2.471(3)	Pb(3)–O(9)	2.624(4)
Pb(2)–O(4)^c	2.565(3)		
N(1)–Pb(1)–O(1)	64.99(10)	O(2)^b–Pb(2)–O(7)	125.92(10)
N(1)–Pb(1)–O(4)	61.40(11)	O(2)^b–Pb(2)–O(12)	80.35(11)
N(1)–Pb(1)–O(6)^a	76.88(11)	O(4)^c–Pb(2)–O(7)	70.01(10)
N(1)–Pb(1)–O(11)	90.17(11)	O(4)^c–Pb(2)–O(12)	83.79(11)
O(1)–Pb(1)–O(4)	95.23(10)	O(7)–Pb(2)–O(12)	152.31(10)
O(1)–Pb(1)–O(6)^a	77.24(10)	N(3)–Pb(3)–O(2)^b	139.70(10)
O(1)–Pb(1)–O(11)	149.32(11)	N(3)–Pb(3)–O(3)	74.34(11)
O(4)–Pb(1)–O(6)^a	136.28(12)	N(3)–Pb(3)–O(8)	71.06(12)
O(4)–Pb(1)–O(11)	87.42(12)	N(3)–Pb(3)–O(9)	64.57(11)
O(6)^a–Pb(1)–O(11)	79.83(12)	O(2)^b–Pb(3)–O(3)	73.15(10)
O(1)–Pb(2)–O(2)^b	93.87(11)	O(2)^b–Pb(3)–O(8)	79.48(11)
O(1)–Pb(2)–O(4)^c	82.76(11)	O(2)^b–Pb(3)–O(9)	154.38(11)
O(1)–Pb(2)–O(7)	95.41(11)	O(3)–Pb(3)–O(8)	78.15(11)
O(1)–Pb(2)–O(12)	71.85(12)	O(3)–Pb(3)–O(9)	131.39(12)
O(2)^b–Pb(2)–O(4)^c	164.04(11)	O(8)–Pb(3)–O(9)	109.85(12)

[a] Symmetry codes: (a) $x - 1, y, z$; (b) $-x, -y, -z$; (c) $-x, -y + 1, -z$.

geometry in which the lone pair occupies the sixth coordination site. The same as for Pb1, one L^{3-} anion is chelated to Pb3 *via* one nitrogen donor (N3), one phosphonate (O8) and one carboxylate oxygen atom (O9). The bond lengths of Pb–O and Pb–N lie in the range of 2.381(3)–2.713(3) and 2.608(4)–2.743(3) Å, respectively. On the other hand, the coordinated and free water molecules provide hydrogen atoms to form hydrogen bondings with nitrogen atoms of pyridine rings and carboxylate oxygen atoms. Furthermore, one carboxylate oxygen atom and the pyridine group of L^{3-} anion do not take part in coordination with Pb ions. This is different from **1**. As a result, both L^{3-} anions exhibit pentadentate modes to combine six and three Pb(II) ions, respectively (Fig. 3b).

Table 4 Hydrogen bond lengths (Å) and angles (°) for **2**[a]

D–H···A	D–H	H···A	D···A	D–H···A
O11-H1···O9^e	0.94(2)	1.86(3)	2.786(5)	168(5)
O11-H2···O13^f	0.94(2)	1.77(2)	2.702(6)	172(5)
O12-H3···O5^c	0.95(2)	1.76(3)	2.693(5)	167(6)
O12-H4···N4^d	0.96(2)	1.91(2)	2.860(6)	168(6)
O13-H5···N2^g	0.95(2)	1.90(2)	2.808(7)	160(5)
O13-H6···O5^h	0.95(2)	1.79(2)	2.716(5)	165(6)

[a] Symmetry codes: (c) $-x, -y + 1, -z$; (d) $x, y, z - 1$; (e) $x - 1, y + 1, z$; (f) $-x, -y + 1, -z + 1$; (g) $x + 1, y, z$; (h) $-x + 1, -y + 1, -z + 1$.

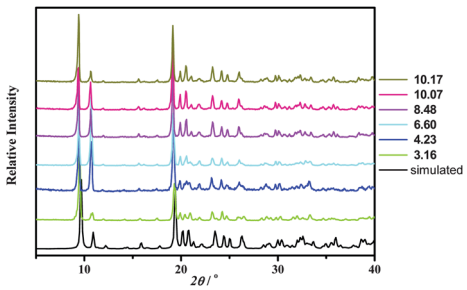

Fig. 1 Powder XRD patterns simulated from single-crystal X-ray data of **1** ,and experimental data of polycrystallites of **1** synthesized at different pH values.

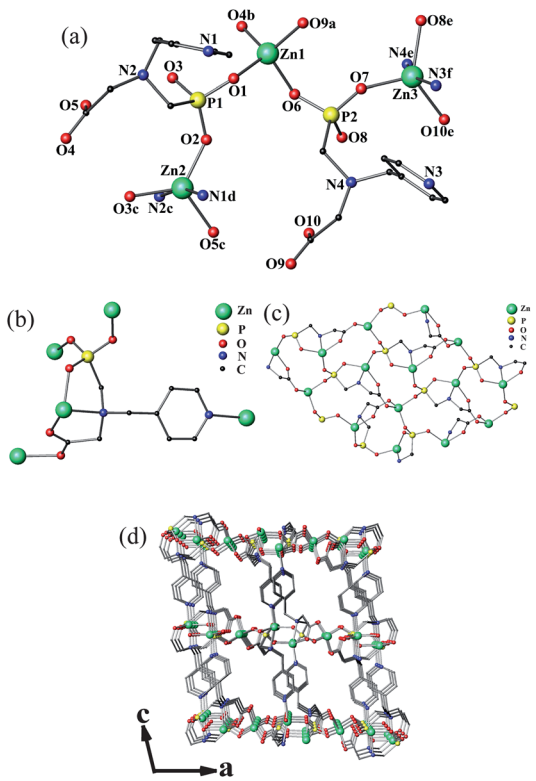

Fig. 2 Ball-stick views of (a) the coordinated environment of Zn(II) ions, (b) coordination modes of L^{3-} anions, (c) the 2D hybrid layer, and (d) the 3D framework in **1**. Unrelated atoms are omitted for clarity. Symmetry codes: *a*: $x, y-1, z$; *b*: $-x, y-1/2, -z+1/2$; *c*: $-x, y+1/2, -z+1/2$; *d*: $-x, -y+1, -z+1$; *e*: $-x-1, y-1/2, -z+1/2$; *f*: $-x-1, -y+1, -z+1$.

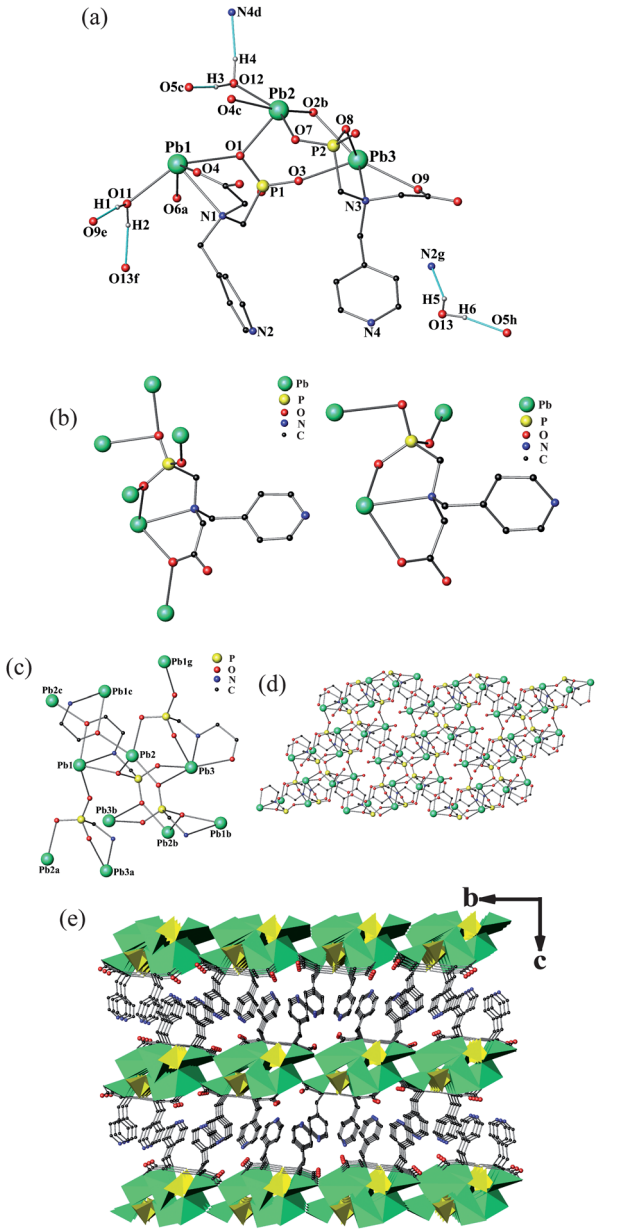

Fig. 3 Ball-stick views of (a) the coordinated environment of Pb(II) ions, (b) coordination modes of L^{3-} anions, (c) the interaction among Pb(II) ions, (d) the 2D hybrid layer, and (e) the 3D structure in **2**. Blue–green lines represent hydrogen bonding. Unrelated atoms are omitted for clarity. Symmetry codes: *a*: $x-1, y, z$; *b*: $-x, -y, -z$; *c*: $-x, -y+1, -z$; *d*: $x, y, z-1$; *e*: $x-1, y+1, z$; *f*: $-x, -y+1, -z+1$; *g*: $x+1, y, z$; *h*: $-x+1, -y+1, -z+1$.

The interactions among Pb ions are rather complicated and are listed as follows. Pb1 contacts with neighboring Pb2 and Pb2c with one phosphonate and one carboxylate oxygen atom, respectively (Fig. 3c). Pb1 also connects Pb3, Pb3a, Pb3b, Pb2a and Pb2b through five –O–P–O– groups, respectively. Pb2 contacts with Pb3 not only through one phosphonate oxygen atom, but also two –O–P–O– groups along with one –O–P–C–N– group. As a result, the distance of Pb2···Pb3 is only 3.821 Å. In addition, Pb2 also connects Pb3b through two –O–P–O– groups, as well as Pb1b, Pb1g and Pb2b *via* three –O–P–O– groups, respectively. Except for the interaction between Pb2 and Pb3, Pb3 contacts with Pb1, Pb1b, Pb1g, Pb2b and Pb3b through seven –O–P–O– and two –O–P–C–N– groups. Thus, the interconnection of Pb ions through phosphonate and carboxylate groups, along with nitrogen atoms of L^{3-} anions, results in a complicated 2D hybrid layer (Fig. 3d), and the hybrid layers are further held together by hydrogen bonding. The non-coordinated pyridine rings are sandwiched between the layers (Fig. 3e).

Thermal stabilities

The thermogravimetric analysis (TGA) for solids **1** and **2** were performed under an air atmosphere. TGA curve of solid

1 illustrates that an obvious stage occurs from room temperature to 200 °C with 4.81% weight loss, which is attributed to the loss of two free water molecules (calculated 4.83%). After solid **1-200** was dipped in water for two days, the TGA curve is the same as that of as-prepared **1**. This result demonstrates that the water molecules can be reversibly removed and recovered. The TGA curve of solid **2** indicates that an obvious stage appears from 100 to 240 °C with 4.59% weight loss due to the loss of one free and two coordinated water molecules (calculated 4.54%). Upon further heating, little weight loss appears until an abrupt stage starts from 390 and 290 °C for solids **1** and **2**, respectively. This is due to the decomposition of L^{3-} groups, resulting in the collapse of their frameworks. This result indicates that the 3D pillared framework of solid **1** behaves more stable than the 2D layer of solid **2**. Furthermore, powder XRD patterns of solid **1-350** are essentially in agreement with those of as-prepared **1**, and the elemental analyses of solid **1-350** is consistent with the calculated value, which unambiguously suggests little change of the framework.

Luminescent properties

No any emission for the ligand, 0.002 M of Na_3L solution and solid **2** can be detected under our experiment. In contrast, solid **1** displays bright purple–blue luminescence with a maximum band at 427 nm upon excitation at 271 nm (Fig. 4a). The lifetime for λ_{em} = 426 nm is 0.98(3) ns. The external quantum yield reaches 8.60% upon excitation at 275 nm. It is worth noting that the bright purple–blue emission can be retained after heating treatment. For example, solid **1-350** can also emit bright purple–blue emission (Fig. 4b).

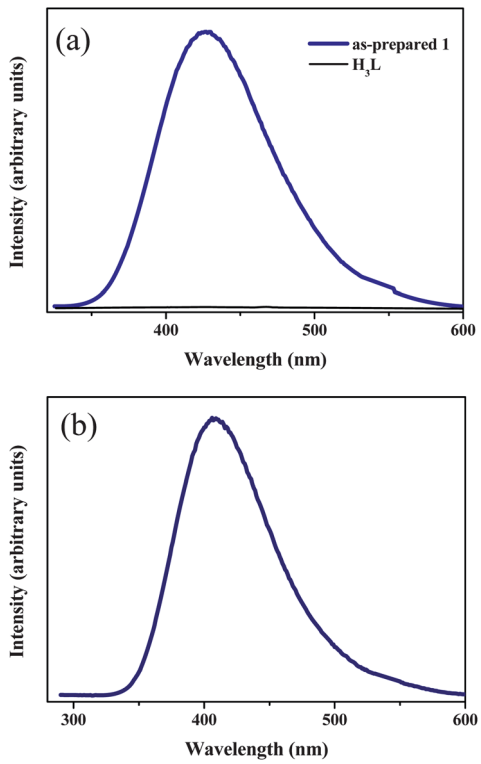

Fig. 4 (a) Relative intensities of emission for solids **1** and $\mathbf{H_3L}$, and (b) emission spectrum of solid **1-350**.

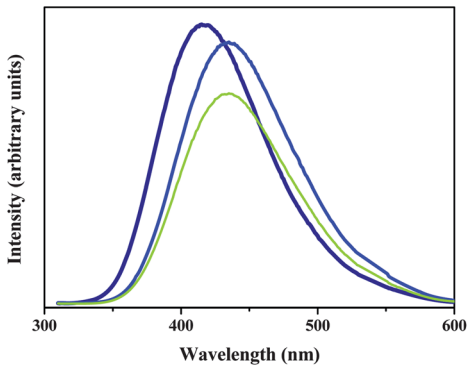

Fig. 5 Relative emission intensities of emission for solid **1-200** (purple), and solid **1-200** which has been exposed to the equilibrated vapors of pyridine (blue) and nitrobenzene (green) for 12 days.

To examine the potential application of the dehydrated solid of **1** for the sensing of small molecules, luminescent emission, IR spectra and elemental analyses were investigated after solid **1-200** was exposed to the equilibrated vapors of pyridine and nitrobenzene for 12 days. Both IR spectra and elemental analyses are the same as those of solid **1-200**. These results are in accord with the small BET surface area of solid **1-200** (1.68 $m^2\ g^{-1}$). Besides a 20 nm red-shift, the luminescent intensity can be weakened by nitrobenzene, which is toxic and readily absorbed through the skin (Fig. 5). Furthermore, after solid **1-200** was exposed to the equilibrated vapors of nitrobenzene for 12 days and then dipped in ethanol, $C_6H_4NO_2^-$ (m/z = 122.4) can be found in the ESI mass spectrum, indicating that a trace of nitrobenzene was adsorbed at the surface of solid **1-200**. The mechanism of luminescent quenching is likely due to the electron-poor nitrobenzene acting as an acceptor in the electron transfer processes.[12]

Conclusions

In summary, we have described the syntheses, crystal structures and properties of two new metal phosphonates, $[Zn_3(L)_2]\cdot 2H_2O$ (**1**) and $[Pb_3(L)_2(H_2O)_2]\cdot H_2O$ (**2**). In **1**, $[ZnO_4]$ tetrahedra and $[ZnO_3N_2]$ trigonal-bipyramids are connected by L^{3-} anions with heptadentate modes to form a 3D pillared framework, while in **2**, L^{3-} anions exhibit pentadentate modes to combine Pb(II) ions into a complicated 2D hybrid layer. Solid **1** is thermally stable up to 350 °C under an air atmosphere. Solid **1** also displays bright purple–blue luminescence, which can be retained after heat-treatment at 350 °C under an air atmosphere.

Acknowledgements

This research was supported by grants from the State Key Laboratory of Structure Chemistry, Fujian Institute of Research on the Structure of Matter, Chinese Academy of Sciences (CAS) and the National Science Foundation of China (21173220, 20801055 and 21073192).

Notes and references

1 A. Clearfield, Metal phosphonate chemistry, in *Progress in Inorganic Chemistry*, ed. K. D. Karlin, Wiley, New York, 1998, Vol. 47, pp. 371–511.

2 (*a*) J. G. Mao, *Coord. Chem. Rev.*, 2007, **251**, 1493; (*b*) J. Wu, H. W. Hou, H. Y. Han and Y. T. Fan, *Inorg. Chem.*, 2007, **46**, 7960; (*c*) N. G. Armatas, W. Ouellette, K. Whitenack, J. Pelcher, H. Liu, E. Romaine, C. J. O'Connor and J. Zubieta, *Inorg. Chem.*, 2009, **48**, 8897; (*d*) R. M. P. Colodrero, A. Cabeza, P. Olivera-Pastor, A. Infantes-Molina, E. Barouda, K. D. Demadis and M. A. G. Aranda, *Chem. Eur. J.*, 2009, **15**, 6612.

3 (*a*) R. B. Fu, S. M. Hu and X. T. Wu, *Cryst. Growth Des.*, 2007, **7**, 1134; (*b*) R. B. Fu, S. M. Hu and X. T. Wu, *J. Solid State Chem.*, 2011, **184**, 159.

4 (*a*) C. I. Yang, Y. T. Song, Y. J. Yeh, Y. H. Liu, T. W. Tseng and K. L. Lu, *CrystEngComm.*, 2011, **13**, 2678; (*b*) V. Baskar, M. Shanmugam, E. C. Sañudo, M. Shanmugam, D. Collison, E. J. L. McInnes, Q. Wei and R. E. P. Winpenny, *Chem. Commun.*, 2007, 37; (*c*) X. G. Liu, S. S. Bao, Y. Z. Li and L. M. Zheng, *Inorg. Chem.*, 2008, **47**, 5525; (*d*) P. F. Wang, Y. Duan, J. M. Clemente-Juan, Y. Song, K. Qian, S. Gao and L. M. Zheng, *Chem. Eur. J.*, 2011, **17**, 3579.

5 (*a*) J. L. Song, F. Y. Yi and J. G. Mao, *Cryst. Growth Des.*, 2009, **9**, 3273; (*b*) D. G. Ding, B. L. Wu, Y. T. Fan and H. W. Hou, *Cryst. Growth Des.*, 2009, **9**, 508; (*c*) T. H. Yang, Y. Liao, L. M. Zheng, R. E. Dinnebier, Y. H. Sua and J. Ma, *Chem. Commun.*, 2009, 3023.

6 (*a*) H. Y. Liu, Z. J. Zhang, W. Shi, B. Zhao, P. Cheng, D. Z. Liao and S. P. Yan, *Dalton Trans.*, 2009, 4416; (*b*) L. R. Guo, F. Zhu, Y. Chen, Y. Z. Li and L. M. Zheng, *Dalton Trans.*, 2009, 8548; (*c*) A. N. Alsobrook and T. E. Albrecht-Schmitt, *Inorg. Chem.*, 2009, **48**, 11079; (*d*) M. Feyand, C. Näther, A. Rothkirch and N. Stock, *Inorg. Chem.*, 2010, **49**, 11158.

7 (*a*) S. F. Tang, J. L. Song, X. L. Li and J. G. Mao, *Cryst. Growth Des.*, 2007, **7**, 360; (*b*) D. K. Cao, J. Xiao, J. W. Tong, Y. Z. Li and L. M. Zheng, *Inorg. Chem.*, 2007, **46**, 428; (*c*) A. N. Alsobrook, B. G. Hauser, J. T. Hupp, E. V. Alekseev, W. Depmeierc and T. E. Albrecht-Schmitt, *Chem. Commun.*, 2010, **46**, 9167; (*d*) A. Zavras, J. A. Fry, C. M. Beavers, G. H. Talboa and A. F. Richards, *CrystEngComm.*, 2011, **13**, 3551.

8 (*a*) J. M. Liang and G. K. H. Shimizu, *Inorg. Chem.*, 2007, **46**, 10449; (*b*) D. K. Cao, Y. Z. Li and L. M. Zheng, *Inorg. Chem.*, 2007, **46**, 7571; (*c*) P. F. Wang, Y. Duan, T. W. Wang, Y. Z. Li and L. M. Zheng, *Dalton Trans.*, 2010, **39**, 10631; (*d*) P. F Wang, D. K. Cao, S. S. Bao, H. J. Jin, Y. Z. Li, T. W. Wang and L. M. Zheng, *Dalton Trans.*, 2011, **40**, 1307.

9 (*a*) R. B. Fu, S. M. Hu and X. T. Wu, *CrystEngComm.*, 2011, **13**, 2331; (*b*) R. B. Fu, S. M. Hu and X. T. Wu, *CrystEngComm.*, 2011, **13**, 6334.

10 G. M. Sheldrick, *SHELXT 97, Program for Crystal Structure Refinement*, University of Göttingen, Germany, 1997.

11 A. W. Addison, T. N. Rao, J. Reedijk, J. van Rijnn and G. C. Verschoor, *J. Chem. Soc., Dalton Trans.*, 1984, 1349.

12 (*a*) S. Shanmugaraju, S. A. Joshi and P. S. Mukherjee, *J. Mater. Chem.*, 2011, **21**, 9130; (*b*) M. E. Kose, B. A. Harruff, Y. Lin, L. Monica, F. S. Lu and Y. P. Sun, *J. Phys. Chem. B*, 2006, **110**, 14032; (*c*) J. S. Yang and T. M. Swager, *J. Am. Chem. Soc.*, 1998, **120**, 5321; (*d*) Y. Liu, R. C. Mills, J. M. Boncella and K. S. Schanze, *Langmuir*, 2001, **17**, 7452.